DIAGNOSIS AND PROGNOSIS OF SLOW SPEED BEARING BEHAVIOUR UNDER GREASE STARVATION CONDITION

Journal:	*Structural Health Monitoring*
Manuscript ID	SHM-16-0224.R1
Manuscript Type:	Original Manuscript
Date Submitted by the Author:	17-Feb-2017
Complete List of Authors:	Elforjani, Mohamed; University of Hertfordshire, Mechanical Engineering
Keywords:	Acoustic Emission, Vibration Measurements, Condition Monitoring, Remaining Useful Life, Slow Speed Bearings, Artificial Neural Network
Abstract:	The monitoring and diagnosis of rolling element bearings with Acoustic Emission (AE) and vibration measurements has evolved as one of the much used techniques for condition monitoring and diagnosis of rotating machinery. Further, recent developments indicate the drive towards integration of diagnosis and prognosis algorithms in future integrated machine health management systems. With this in mind, this paper is an experimental study of slow speed bearings in a starved lubricated contact. It investigates the influence of grease starvation conditions on detection and monitoring natural defect initiation and propagation using AE approach. Further, the experiment is aimed at a comparison of results acquired by AE and vibration diagnosis on-full scale axial bearing. In addition, the paper also concentrates on the estimation of the Remaining Useful Life (RUL) for bearings whilst in operation. To implement this, a multilayer Artificial Neural Network model (ANN) has been proposed to correlate the selected AE features with corresponding bearing wear throughout laboratory experiments. Experiments confirm that the obtained results were promising and selecting this appropriate signal processing technique can significantly affect the defect identification.

DIAGNOSIS AND PROGNOSIS OF SLOW SPEED BEARING BEHAVIOUR UNDER GREASE STARVATION CONDITION

Mohamed Elforjani

University of Hertfordshire,
School of Engineering and Technology,
College Lane Campus, Hatfield, AL10 9AB, UK
elforjani@gmail.com or m.elforjani@herts.ac.uk

ABSTRACT

The monitoring and diagnosis of rolling element bearings with Acoustic Emission (AE) and vibration measurements has evolved as one of the much used techniques for condition monitoring and diagnosis of rotating machinery. Further, recent developments indicate the drive towards integration of diagnosis and prognosis algorithms in future integrated machine health management systems. With this in mind, this paper is an experimental study of slow speed bearings in a starved lubricated contact. It investigates the influence of grease starvation conditions on detection and monitoring natural defect initiation and propagation using AE approach. Further, the experiment is aimed at a comparison of results acquired by AE and vibration diagnosis on-full scale axial bearing. In addition, the paper also concentrates on the estimation of the Remaining Useful Life (**RUL**) for bearings whilst in operation. To implement this, a multilayer Artificial Neural Network model (**ANN**) has been proposed to correlate the selected AE features with corresponding bearing wear throughout laboratory experiments. Experiments confirm that the obtained results were promising and selecting this appropriate signal processing technique can significantly affect the defect identification.

Keywords: Acoustic Emission, Vibration Measurements, Condition Monitoring, Remaining Useful Life, Slow Speed Bearings, Artificial Neural Network.

1   INTRODUCTION

A tremendous amount of work has been undertaken over the last 30-years in developing of the application of the condition monitoring techniques for bearing health monitoring [1]. Although a lot of work has been undertaken in the area of bearing fault diagnosis,

1

there is still an on-going need for the area of bearing prognosis. Most of the techniques that are widely used for health monitoring and prediction of RUL are divided into two models [2]. The first model is the model based (or physics-based) method, which predicts the RUL based on the propagation of the damage mechanism. The second approach involves the data driven methods. In this model, data acquired by sensors are further processed in relevant models (parametric/non-parametric) to estimate the RUL [3]. To use the data driven models, sufficient failure data should be provided to train the prediction models such as Neural Networks, Bayesian Networks and Markova Processes. Over a number of recent years, attempts to estimate the remaining useful life of bearings have been addressed in number of publications.

Nathan et al. [4], for instance, undertook experimental bearing tests to predict the RUL of an aircraft engine bearing. In this study a model based on the steps of developing the spall propagation mechanism was used. To validate the results of the developed RUL prediction method, a full-scale bearing test was performed. It was postulated that the developed model could accurately predict the spall propagation and the corresponding RUL. Shao et al. [5] proposed Progression Prediction of Remaining Life (PPRL) of bearing. In this model, different prediction methods were applied to different bearing running stages. Another model, Neural Network based, for predicting bearing failures was developed by Gebraeel et al. [6]. Gebraeel came up with a conclusion that best estimation of bearing failure times can be obtained by weighted average of the exponential parameters. In his PhD study, Ghafari [7] extracted vibration signals features that were used as the input of the diagnostic model. Adaptive Neuro-Fuzzy Inference System (ANFIS) was used to evaluate the efficiency of bearing prognosis. It was reported that the trained ANFIS could successfully capture the damage propagation behaviour and predict the future states of the same series of bearings at different speed and load conditions.

Comparative investigation of the accuracy between three different techniques to estimate the bearing RUL was done by Sutrisno et al. [8]. Moving Average Spectral Kurtosis and Bayesian Monte Carlo, Support Vector Regression and Anomaly Detection have been applied to an experimental data set from seventeen ball bearings provided by the FEMTO-ST Institute. Sutrisno reported that Anomaly Detection

2

method was found to be the most accurate method overall. Goebel et al. [9] undertook another comparative results between Relevance Vector Machine (RVM), Gaussian Process Regression (GPR), and a Neural Network model. Obtained results showed that each algorithm produced a significant different estimation of RUL from the others. A machine prognostics model based on health state estimation using Support Vector Machines (SVM) has been proposed in an undertaken investigation by Kim et al. [10]. Data from faulty bearing cases in pumps, used for High Pressure Liquefied Natural Gas (LNG), were analysed. Results were used to identify the failure degradation process and further validate the feasibility of the proposed model for accurate assessment of RUL.

An artificial neural network (ANN) based method was developed by Tian [11]. Features such as age and multiple condition monitoring measurements at the present and previous inspection points were employed as inputs for the proposed model. Based on these inputs the ANN model produced the bearing life percentage as the output. Tian reported that achieving accurate useful life prediction using the proposed method was observed. Another ANN model based on the data driven prognostic method was proposed by Ben Ali et al. [12]. In this proposed model, Weibull Distribution (WD) along with the Simplified Fuzzy Adaptive Resonance Theory Map (SFAM) neural network was employed to estimate the bearings RUL. To fit and avoid the fluctuation in the measured time domain data, a modified Weibull Distribution function was selected. Features at present and previous inspection time points were first extracted from the time domain signals and then fitted using the selected WD. Fitted RMS, kurtosis and Root Mean Square Entropy Estimator (RMSEE), a fault indicator that was proposed by the authors, were used to train the SFAM. It is worth mentioning that for the accuracy assessment the proposed model was also applied to unfitted data. It was postulated that the proposed technique could reliably predict the RUL and can be expanded to include the prognosis of the other mechanical components.

Mejia et al. [13] utilized Wavelet Packet Decomposition (WPD) and Gaussians Hidden Markov Models (MoG-HMM) to estimate the bearing RUL. WPD was used to extract the relevant information from the vibration bearing signals. These features are then used to train several behaviour models of MoG-HMM at different initial states and operating conditions of the bearing. Comparative results between the estimation of RUL using the

3

extracted time domain features and the extracted time-frequency domain features was also presented. Mejia came up with a conclusion that is the extracted features from time-frequency domain are more precise in achieving the RUL. In another investigation, Loutas et al. [14] has presented another approach for condition assessment and life prediction. This method is mainly based on nonlinear Support Vector Regression (SVR) where a set of multiple statistical vibration features from the time domain, frequency domain, and time scale domain through a wavelet transform features were extracted. Further, the authors also utilized Wiener Entropy (WE) for the condition monitoring of rolling bearings. Prior to testing, the SVR model was trained and tuned off-line using the extracted features. Unseen data was then employed to online RUL prediction. The authors claimed that the results obtained by the proposed model showed a significant consistency with the corresponding actual bearing degradation level.

The monitoring and diagnosis of rolling element bearings with the high frequency Acoustic Emission (AE) technology has been on-going since the late 1960's [15]. Jamaludin et al [16] conducted an experimental work for monitoring of slow-speed rolling bearing using stress waves. This study presented an investigation into the applicability of stress wave analysis for detecting early stages of bearing damage at a rotational speed of 1.12 RPM (0.0187Hz). Attempts had been made to generate a natural defect onto the bearing components by fatiguing. However, after allowing the test bearing to operate for a period of 800 hours, while under conditions of grease starvation, no defect and/or wear was visually detectable on any of the bearing components. This was attributed to the low speed phenomena of 1 RPM and lack of contaminants to initiate and accelerate defects. In further study, Morhain et al [17] examined the application of standard AE characteristic parameters on a radially loaded bearing. The use of typical AE parameters such as RMS and counts was validated as a robust technique for detecting bearing damage. This study determined the most appropriate threshold level for AE counts diagnosis, the first known attempt.

Al-Ghamdi et al [18] conducted a comparative experimental study on the use of Acoustic Emission and vibration analysis for bearing defect identification and estimation of defect size. This study showed that AE can offer earlier fault detection and improved identification capabilities than vibration analysis. Furthermore, the AE

4

technique also provided an indication of the defect size, allowing the user to monitor the rate of degradation on the bearing; unachievable with vibration analysis. In another work, Miettinen et al [19] described the use of the acoustic emission method in the monitoring of faults in an extremely slowly rolling bearing. The study contains the results of AE measurements where the rotational speed of the shaft was from 0.5 RPM to 5 RPM. The measurements were carried out using a laboratory test rig with grease lubricated spherical roller bearings of an inner diameter of 130 mm and a load of 70 kN. Prior to testing the test bearing had been naturally damaged on its outer race during normal use in industry. Choudhury et al [20] undertook a work for the detection of defects in roller bearings using Acoustic Emission. Defects were simulated in the roller and inner race of the bearings by the spark erosion method. AE of bearings without defect and with defects of different sizes has been measured.

To date most published work on the application of the AE to monitoring bearing mechanical integrity have been conducted on artificially ('seeded') damage or ground metal debris that were introduced gradually into bearings. Few attempts were made to assess the potential of the Acoustic Emission (AE) technology for detecting natural cracks. Price et al. [21] showed the applicability of AE to monitor naturally generated scuffing and pitting defects in a four ball lubricant test machine. The work undertaken by Yoshioka [22] also identified the onset of natural degradation in bearings with AE. It is worth mentioning that Yoshioka employed a bearing with only three rolling elements which is not representative of a typical operational bearing. Moreover, Yoshioka terminated AE tests once AE activity increased as such the propagation of identified subsurface defects to surface defects was not monitored.

The only published work by Elforjani et al [23, 24, 25 and 26] could be considered the first that directly addressed not only the identification of the initiation of natural cracks, but also its propagation to spalls or surface defects on a conventional slow speed bearing with the complete set of rolling elements. Elforjani also showed the significant advantages of AE over the well-established vibration monitoring technique in detecting the loss of mechanical integrity at early stages [23]. However, to speed up natural crack initiation, Elforjani employed a combination of a thrust ball bearing and a thrust roller

5

bearing. One race of ball bearing (SKF 51210) was replaced with a flat race taken from the roller bearing (SKF 81210 TN) of the same size.

The useful operating life of a rolling element bearing is influenced by a number of factors. Some of the factors are controlled by the designer while others are controlled by the user. For instance, in the rolling bearing there is always a slight slippage between the rolling elements and bearing ring. The rolling element is separated by a lubricant in the bearing ring. To keep machines functioning at optimal levels, failure detection in a starved lubricated contact must be investigated. Also, off the shelf, most of the published attempts, for earlier bearing prognosis, have made use of vibration analysis, in which the current and previous vibration data was used to predict the RUL of bearings. There are potentially unlimited opportunities for a wide scope to develop methods, tools and applications for effective prognostic systems. Keeping this in mind, this work builds further on the work of Elforjani by monitoring the initiation and propagation of natural cracks on slow speed bearing under grease starvation conditions and estimating the remaining useful life for real world slow speed bearings.

2   EXPERIMENTAL PROCEDURE AND EQUIPMENTS

A specially designed test rig that encouraged the natural damage condition of a test bearing was employed. To speed up crack initiation, a very small amount of lubricant has been added to a thrust ball bearing (SKF 51210), shown in figure 1. It is worth mentioning that this small amount of grease was neither weighed nor its thickness was measured; just a random small amount of grease was added to the bearing ring prior to testing. The reason behind this is to simulate the real world applications where the measurements or prediction of the amount of lubricant inside the bearing, whilst in operation, are very challenging. This is due to the accessibility problems such as bearing location and/or bearing geometry. Further, very sophisticated and costly devices are required to carry out the oil and lubricant analysis that is very often undertaken offline. As a result of that, this approach allowed the test bearing to operate under conditions of grease starvation within a few operating period depending on the load condition before natural fatigue could be initiated on the bearing cage.

6

Figure 1 Test Bearing

The test-rig, presented in figure 2, was employed for this investigation. It consisted of a hydraulic loading device, an eclectic motor (MOTOVARIO-Type HA52 B3-B6-B7 j20, 46-Lubricated: AGIP), a coupling and a supporting structure. The test bearing was positioned between the stationary thrust loading shaft and the rotating disk which housed one of the bearing races. The second race was fitted onto the loading shaft in a specifically designed housing. This housing was constructed to allow for placement of AE sensor and thermocouple directly onto the bearing race. The thrust shaft was driven by a hydraulic cylinder (Hi-Force HYDRAULICS-MODEL No: HP110-HAND PUMP-SINGLE SPEED-WORKING PRESSURE: 700 BAR) which moved forwards to load the bearing and backwards for allow periodical inspections and replacements of the test bearing. The rotating disk was driven by a shaft attached to the motor with an output speed of 72 rpm. A thrust bearing (SKF 81214 TN) was placed between the coupling and the test bearing to react the axial load. A coupling system was carefully selected to absorb any vibration as a result of attaching the shaft to the motor.

Figure 2 Test Rig Layout

The AE acquisition system, shown in the above figure, employed commercially available piezoelectric sensor (Physical Acoustic Corporation type "PICO") with an operating frequency range of 200-750 kHz at temperature ranging from -65 ^{o}C to 177 ^{o}C. One acoustic sensor, together with one thermocouple (RoHS-Type: J x 1M 455-4371) were attached to the back of the stationary raceway using superglue. To measure the vibration in the axial direction, one accelerometer (ENDEVCO-236-M-ISOEASE-PF44), was attached to the housing of the stationary bearing race. This accelerometer was connected to the data acquisition system via a vibration meter, see figure 2-2. The acoustic sensor was connected to the data acquisition system through a preamplifier, set at 40 dB gain. The system was continuously set to acquire AE waveforms at 2 MHz sampling rate. During testing AE, vibration and bearing temperature parameters were recorded in a continuous mode. The AE absolute energy and RMS were acquired at a sampling rate of 100 Hz and over a time constant of 10^{-3} seconds. The absolute energy is a measure of the true energy and is derived from the integral of the squared voltage signal divided by the reference resistance (10 k-ohms) over the duration of the AE

7

signal. An average value of bearing temperature over a time constant of 100 seconds throughout the test period was recorded.

3   BEARING TESTS

Under normal conditions of rotational speed, load, good alignment and grease starvation conditions, natural damage begins with small cracks, located on the rolling elements cage, which generated detectable AE signals. For this particular paper four experimental cases are presented that reflect the general observations associated with experimental tests at loads ranging from 20, 25, 30 and 35 kN. The tests were terminated once a significant rise in AE levels, vibration and temperature measurements, was observed. This led to different test periods based on the operating conditions. In addition to the load and operation under grease starvation conditions, this variation might also be attributed to issues such as misalignment, unbalance, etc; however, best efforts were made to minimise this.

Observations of continuous monitoring of the AE levels, in addition to vibration and bearing temperature parameters are presented in figures 3 to 6. At the end of the test (7200 seconds and Load = 35 kN) there was visible surface damage on the bearing cage. It was observed that at approximately 4320 seconds into operation AE levels began to increase steadily. This was not observed on the vibration measurements though vibration levels increased after 5760 seconds of operation; much later that was detected by AE, reinforcing the widely acknowledged view that AE is more sensitive than vibration for bearing defect identification [23]. The increase in AE energy levels from earlier in the test run between 720 to 2160 seconds to the condition of damage was in the order of 600%, presented in figure 3. The percentage of the increase in AE levels in the load cases of (20, 25 and 30 kN) was about 400%, 900% and 600% respectively.

After run-in stage in the low load cases (30, 25 and 20 kN), all measured AE and vibration parameters remained almost constant. Significant increase in AE activity from 5400, 8000 and 8000 seconds of operation was observed whilst vibration measurements showing transient increase at 7200, 12000 and 11000 seconds of operation in the load cases of 30, 25 and 20 kN respectively, shown in figures 4 to 6. Observations from figures also reinforce the global opinion that AE tends to be noisy and spiky when

8

the well-developed defect is pronounced whilst the vibration steadily increases due to the excitation of the natural structural frequency of the system component. Also continuous monitoring of AE activity showed that the onset of the significant rise in AE levels was earlier observed in the load case of 20 kN than the load case of 25 kN, see figures 5 and 6, reinforcing the acknowledged view that the variation in actual test period leading to fully developed damage on the bearing was unpredictable.

It is also worth mentioning that simultaneous recording of bearing temperature from the thermocouple channel attached to the back of the stationary bearing raceway stabilised at an average of 35°C after the run-in stage. The measurement of temperature was undertaken to assess the consistency of lubricant viscosity throughout the test period. The significant variation in the trend of this indicator will also help to identify whether the friction properties between the bearing elements are relatively constant or not. On the termination of tests a maximum temperature of 46°C for the load cases of 35 and 30 kN was recorded whilst lower temperature value of 36°C on the termination of tests was registered for the load cases of 25 and 20 kN, see figures 3 to 6. On termination of the tests, a visual inspection revealed a severe surface damage on the bearing cage, see figure 7. This suggested that there was a slippage between the rolling elements and the bearing rings as a result of the starving lubricant contact, which greatly increased the pressure, friction and wear and eventually reduced the bearing life.

Figure 3 Test Conditions Case I (Load 35 kN)

Figure 4 Test Conditions Case II (Load 30 kN)

Figure 5 Test Conditions Case III (Load 25 kN)

Figure 6 Test Conditions Case IV (Load 20 kN)

Figure 7 Surface Damage on the Bearing Cage

Observations of the AE waveforms, sampled at 2 MHz showed changing characteristics as a function of time. These AE waveforms, associated with the observations of the bearing test shown in figure 3, are presented in figures 8, where a typical AE waveform associated with spurious AE transient events is presented after 4320 seconds of

operation. The waveform at this time of operation shows an AE transient bursts this is attributed to the onset of 'less mature' damage on the bearing. At 7200 seconds operation, significant AE transient events associated with the fully developed defect on the bearing are clearly noted, see figure 8. This highlighted the fact that AE waveforms are just as sensitive to changes in bearing mechanical state as the continuous measurement of AE energy.

As surface defects on the bearing cage, such as spalls, are continually developing it is postulated that a newly formed spall will contribute relatively higher AE events as the edges of this newly formed defect will be rougher in comparison to an already existing spall which becomes smoothened with the passage of time. This assumption was made based on the several tests undertaken prior to the reported cases. Results from these pre-tests along with the visual inspection showed that significant rise in AE, vibration and temperature is a clear indication of new formed spalls on the bearing cage. This also explains the sharp bursts of AE activity noted during observations of continuously monitored AE energy levels, see figure 3. Even though the overall levels are increasing from 4320 seconds, relatively large transient rises were noted during the period from 5040 seconds to 7200 seconds. The author believes that these large transient burst are attributed to regions that have newly developed surface damage; this is an evolutionary process giving rise to peaks and troughs in AE levels.

Figure 8 AE Waveforms associated with 35 kN Load (Onset Rise of AE Levels until the Termination)

4   ESTIMATION OF REMAINING USEFUL LIFE (RUL)

Thus far the observations have shown AE to monitoring the degradation of an accelerated test. In this section the methodology, used for estimation the remaining useful life (RUL) of the test bearings, is presented. The feature extraction, classification, and prediction are also discussed.

4.1　EXTRACTION AND REDUCTION OF AE FEATURES

In the application of the condition monitoring, signals are information provider. Hence, it is global acceptance that more failure histories will lead to accurate results. The acquired data normally tend to be high dimensional noisy data, such as the case of AE data, and therefore it is necessarily needed to be cleaned, reduced and pre-processed prior to further processing. However, excess in cleaning, reduction and pre-processing the acquired data may lead to lose the significance of the carrying information. Operators are, very often, careful in selecting representative fault index tools to interpret the signal trend. It was thought prudent to ascertain which processing techniques could employ the transient characteristics noted thus far in determining the bearing mechanical condition. Based on the assumption that a feature that monotonically increases over time is the ideal degradation signal [8], the author selected AE RMS along with a new dimensionless fault indicator technique; Signal Intensity Estimator (SIE), proposed by the author.

4.1.1　SIGNAL INTENSITY ESTIMATOR (SIE)

Whilst the Root Mean Square (RMS) is one of the widely used statistical parameters for condition monitoring measurements, it is typically recorded over a predefined time constant. As such the RMS values, for the case of denser data such as AE data, are not necessarily sensitive to transient changes, which typically are of a few micro-seconds. To overcome the inadequacy in the use of the RMS, a relatively more sensitive and robust technique based on the cumulative sums has been proposed; the Signal Intensity Estimator (SIE).

SIE can be defined as the ratio of the sum of cumulative sum of a defined segment, window, ($SCS_{segment}$) in a given signal to the overall sum of cumulative sum ($SCS_{overall}$) of the same signal. This ratio is then multiplied by a magnification factor (MAGF). The advantage of the dimensionless SIE is that it can reduce the complexity of the problem as its result is numerical values without physical dimensions. This in turn will allow the user to perform any analysis for any condition monitoring data (e.g. vibration, AE, etc.) irrespective of their physical units. The SIE envelops the data without losing the information carried by the signal. The advantage of the SIE over the classical

11

envelope and the other parameters is that the SIE is a normalised piecewise segment technique whilst the envelope is based on the entire signal. This means that the SIE dose not only display the ratio of the total at any given time but also it can chart statistic that involves current and previous data values from the process. This helps to track how the sample values deviate from a target value and also improves the ability to detect micro-changes. Besides it resolves the problem in the cases of small values of the calculated SIE, the MAGF also plays a vital role to overcome the problem of selecting the size of a given window. The author assumed that there is a direct proportionality between the MAGF and the selected number of the windows (W). This means the higher number of W the higher MAGF and vice versa. This proportionality produced a constant (k) that is highly dependent on the type of the data. For high dimensionality data, such as the case of continuous acquiring of AE data, high W and small k are preferred whilst small W and high k are better for low dimensionality measurements. Mathematical expressions that are required to perform the SIE analysis are explained as following:

1. To obtain optimal SIE value, signal should be rectified as the first step.
2. The Signal Intensity Estimator (SIE) is calculated using the following equation:

$$SIE = \frac{SCS_{segment}}{SCS_{overall}}.MAGF$$

(1)

3. With the knowledge of the size of a given signal (N) and the size of each segment (n), the MAGF can be derived as:

$$MAGF \; \alpha \; W \tag{2}$$

$$where \; W = \frac{N_{overall}}{n_{segment}} \tag{3}$$

4. With the use of the proportionality constant (k), the MAGF can **simply be calculated** as:

12

$$k = \{2,3,4,5,6,......\} \tag{4}$$

$$MAGF = k.W \tag{5}$$

$$where \begin{cases} k = 2 \ for \ very \ high \ W \ and \ high \ \dim entionality \ data \\ 2 < k < \ 4 \ for \ high \ W \ and \ high \ \dim entionality \ data \\ 4 \leq k \leq 6 \ for \ low \ W \ and \ low \ \dim entionality \ data \\ k > 6 \ for \ very \ low \ W \ and \ low \ \dim entionality \ data \end{cases}$$

It is worth mentioning that the above values of k have been suggested based on the results of the iterative process, undertaken, to achieve the optimal values. Further, these values are used for the continuous monitoring of the degrading bearing whilst large values of k are used for the analysis of waveforms. In application, SIE value of one, between two adjacent segments, is associated with non-transient type signals and greater than one where transient characteristics are present. Selection the size of the segment was justified by an iterative process. For this particular investigation AE signals, recorded throughout the bearing tests, were split into several windows each of which contains 20 segments and the optimal value of k was found to be 4.

The trend of SIE was completely consistent with the general trend of AE energy presented in figures 3 to 6. Steady trend of AE energy, SIE and RMS noted in the termination of the tests is due an already existing spalls, which became smoothened with the passage of time, see figure 7, and will not contribute relatively higher AE events until newly defect is formed. This confirms the author's belief that the SIE is reliable, robust and sensitive to the detection of incipient cracks and surface spalls. It can successfully be employed for condition monitoring of rotating machines.

4.1.1.1 CORRELATION COEFFICIENT

The next phase of this investigation involved the ascertainment of how strong the monotonic relationship is between the SIE and the time duration of the tests. To implement this, what-so-called correlation coefficient was calculated using Pearson's Product-Moment Correlation. In general, correlation can be defined as a class of statistical relationship between variables. From the results presented in **table 1**, it can be

13

seen that true correlation between SIE with time is not equal to 0. From p-value that is less 0.05 and the positive sign of the correlation coefficient, it can be concluded that SIE is strongly correlated with time; association between these two parameters are strong (Strong Monotonic Relationship).

Table 1 Correlation Analysis

4.2 FITTING OF AE SIGNAL FEATURES

As mentioned in the previous section that the acquired data is accompanied with an external noise that significantly influences the final interpretation of the general trend. Although it was observed in the previous sections that the bearing failure, throughout testing period, was relatively a monotonic process, the acquired data cannot be directly fed to the prediction models. This is because that any noise in the acquired data will significantly disturb the performance of the model and subsequently its capability to accurately predict the health condition of the bearings; prediction models in such a case will follow the randomness. To overcome this issue, the raw data have to be fitted using appropriate mathematical functions. To represent trends in the degradation signals, originating from bearings, linear or exponential models were widely employed. In this research work, several linear and exponential function have been applied to the acquired data. Finally, the following exponential sigmoid model was proposed to fit the extracted features first, and then use the fitted values as inputs to the prediction model.

$$f = y_0 + \frac{a}{1 + e^{-\left(\frac{t - x_o}{b}\right)}} \tag{6}$$

This function could fit the different bearing cases that used for constructing, training, validation and testing the prediction model. In the above function f is the magnitude of the signal feature; here (f) is the value of SIE and/or RMS, (a, b and x_o) are the model constants, and (t) is the time. The constant (y_o) is used here to indicate the value when the degradation time is equal to zero. To find the optimal values for the above function constants a, b, x_o and y_o that can fit all the tested measurement series, the popular least-square method was applied to the four bearing cases; figures 9 and 10 show the fitted

14

bearing cases. These cases will be used for constructing, training and validating the prediction model, see the following sections. Tables 2 and 3 also summarize the general optimal estimated constants and global goodness of fit for the exponential model.

Figure 9 Actual and Fitted SIE

Figure 10 Actual and Fitted RMS

Table 2 Estimated Constants for the Exponential Model

Table 3 Global Goodness of Fit for the Exponential Model

Results from the fitted data and parameters of global goodness of fit showed that the suggested model could well fit the extracted SIE and RMS values, see figures 9 to 10 and table 3.

4.3   MULTILAYER ARTIFICIAL NEURAL NETWORK (ANN)

Artificial Neural Networks (ANN) are a supervised machine learning type. They are inspired by biological neural networks and each neuron is represented by a node [27]. It is basically a directed graph where each edge has a weight. These neural networks are capable of learning by changing the weights of their connections [28 and 29]. Components of ANN is defined as the Neural Network Architecture, which involves input neurons, output neurons, hidden neurons, and bias neurons. The input neurons has no processing and are used to provide input signals. On the other hand, output neurons process the units and are used to get the output. The task of the hidden neurons is to add additional processing for the units to achieve a converged solution. The bias neurons are employed to avoid zero results even if the inputs are zero.

It is worth mentioning that the bias neurons are not connected to the input neurons and normally their values set to one. Neurons are connected with each other through a connection weights (synaptic weights) that are used to signify the strength of the connection and therefore, the higher the weight the higher strength of that connection [30]. This will also lead to higher of the effect of the processing. The edge weights have

15

a random value at the beginning and they are updated accordingly. The connection between the neurons is directional, namely, connection from, for instance n1 to n2 is different from the connection from *n2* to *n1* [30]. In general there are two kinds of neural networks; Hopfield Neural Network and Feedforward Neural Network. In the former each neuron is connected to every other neurons whilst there are directed edges from input layer to hidden layer and from hidden layer to output layer in the latter [30]. In the ANN structure, activation functions, for example linear function, hyperbolic tangent and/or sigmoid functions, are extensively also used. These functions take some weights of the input signals and perform some actions.

The model is called a trained model when the weights were adjusted for minimum error (*E*). There are two types of errors; local error and global or network error. The local error is the difference between the ideal value and the actual value whereas the global error is a cumulative effect of all local errors. In the training process, interconnection weights are adjusted so that the global error is less than some Predefined Level (PL). This predefined limit is very sensitive as in the case of a high limit the model will be under trained whilst low limit will lead to over trained model. For the training purpose, different algorithms with different rules to update weights; different calculation methods for global errors and different flow charts, are used. The most common training algorithms include Back-Propagation algorithm, Resilient-Propagation algorithm, Quick-Propagation algorithm and LMA algorithm [30 and 31]. The algorithm terminates the training process when the network error rate is small. To select an appropriate training algorithm, accuracy, required computational resources and training time must be considered.

In this research work, an ANN model was proposed to estimate the RUL for slow speed bearings. The model is a Feedforward ANN model with three layers at beginning that were used for constructing the ANN model; one input layer, one output layer and one hidden layer with changeable number of neurons in the hidden layer. The model parameters such as the number of hidden layers, algorithm type and learning rate were kept changing until the best performance was achieved. The best results eventually were obtained by an ANN model containing one input layer with two inputs parameters; represents the SIE and RMS values, one output layer; represents the estimated RUL,

16

and three hidden layers with seven neurons in the first layer, three neurons in the second layer and seven neurons in the third layer. For the best training, the Resilient Back-Propagation algorithm and the activation sigmoid function (logistic) were selected.

The SIE and RMS were calculated from the acquired AE data and further fitted prior to the training process. The challenging question was that is the proposed SIE a good choice for predicting RUL. Hens, a feasibility study or assessment was conducted for three different ANN models. The first model involved the RMS and SIE as inputs to the ANN model. The second model included SIE as a solely input whereas the third model employed RMS only. The load case of 20 kN was selected to train the three ANN models and the fitted data was passed to the models. The selected algorithm in turn started to train the model. Several runs accompanied with adjusting and tuning the ANN parameters such as weights, number of hidden layers etc. were made to minimize the global error. Eventually, the used algorithm terminated the training process once the error approached almost zero value (it recorded the minimum value). The minimum registered error was 2.8, 2.5 and 8.4 for ANN model with two inputs, ANN model with SIE and ANN model with RMS respectively. The next phase involved validating the trained models. This implemented by passing the fitted data from the load cases (35, 30 and 25 kN) to the trained models. The steps followed from the training of the proposed ANN model until the estimation of the RUL are presented in **figure 11**. Figures 12 to 14 show the final structure of the proposed ANN models that used to estimate the bearing RUL.

Figure 11 Schematic of the Proposed ANN Model

Figure 12 ANN Structure (Two Inputs RMS & SIE)

Figure 13 ANN Structure (One Input SIE)

Figure 14 ANN Structure (One Input RMS)

The RUL, the Error and Sum of Square Error (ESS) were calculated using the equations 7, 8 and 9 respectively.

$$RUL = t_f - t_c \qquad (7)$$

$$Error = \frac{Actual\left(RUL\right) - Estimated\left(RUL\right)}{Actual\left(RUL\right)} \; x \; 100 \tag{8}$$

$$Some\; Square\; Error\left(ESS\right) = \frac{1}{2} \sum_{i=1}^{n} Error_i^2 \tag{9}$$

Where (t_f) is the time at which the fully mature failure is formed, for more details; in this particular investigation this time was selected as the termination of the test period. The (t_c) is the current time at which the RUL is estimated. Results from ANN analysis are detailed in figures 15 to 17 and table 4. By visually inspecting the plots, it can obviously be observed that the predictions made by the ANN model with only SIE as input are almost concentrated around the actual RUL line (a perfect alignment with the line would indicate a low Sum Square Error (ESS) and thus an ideal perfect prediction), whilst obvious difference and poor performance by the ANN model used RMS only as input was observed, see figure 17. Also was noted that the performance of the ANN model with two inputs, SIE and RMS, has been influenced by the RMS values, see figure 15.

Figure 15 ANN Results (Two Inputs RMS & SIE)

Figure 16 ANN Results (One Input SIE)

Figure 17 ANN Results (One Input RMS)

Table 4 summarizes the error analysis where it can be seen that the obtained results ascertain the feasibility of the proposed SIE as a representative input for the ANN model. It can be seen that the lowest error values for the three tested cases (35, 30 and 25 kN) registered by the ANN model with SIE as input. For instance, ESS for the load case of 35 kN was found to be 5237 using the ANN model with SIE whilst 6458 and 8358 were registered by ANN model with two input and by ANN model with RMS respectively. Also interestingly observations were that some negative error values were recorded by different ANN models, figures 15 to 17. These negative values imply that the ANN models have overestimated the RUL. Results also showed that the maximum

prediction error (21.65%) has occurred in the load case of 20 kN using ANN model with RMS as input.

Table 4 Error Results

5   CONCLUSION

Bearing run-to-failure tests under grease starvation conditions were successfully performed. These tests demonstrated the applicability of AE in detecting crack initiation and propagation on bearing cages whilst in operation. The four cases presented are representative of other tests performed in this study and show that there is a clear correlation between increasing AE energy levels and the natural propagation and formation of bearing defects. The study demonstrated that AE parameters such as energy are more reliable, robust and sensitive to the detection of incipient cracks and surface spalls in slow speed bearing than vibration analysis.

RUL for slow speed bearing under starved lubricant contact conditions was also successfully estimated using supervised machine learning techniques. It was shown that the proposed ANN model with Back-Propagation learning could accurately estimate the RUL for slow speed bearings. It can be concluded that the use of ANN as early alarm tools not only minimizes the wasteful machine downtime but also the untimely replacement of components. The study also showed that the continuous monitoring of bearings employing a technique such as the SIE would offer the operator a relatively more sensitive tool for observing high transient type activity. This study can be considered as the first investigative step since it concerns a single application of the proposed models (ANN) to a specific test rig and to unique specimens and therefore its effectiveness, both technically and economically, has to be proved with further investigations.

REFERENCES

1. Jammu, N.S., Kankar, P.K.: A Review on Prognosis of Rolling Element Bearings. International Journal of Engineering Science and Technology (IJEST), ISSN: 0975-5462, Volume 3, Issue10 (2011)

2. Zhigang, T.: An Artificial Neural Network Method for Remaining Useful Life Prediction of Equipment Subject to Condition Monitoring. Journal of Intelligent Manufacturing, ISSN: 0956-5515, Volume 23, Issue 2 (2012)

3. Medjaher, K., Tobon-Mejia, D.A., Zerhouni, N.: Remaining Useful Life Estimation of Critical Components with Application to Bearings. IEEE Transactions on Reliability, Institute of Electrical and Electronics Engineers, DOI: 10.1109/TR.2012.2194175, Volume 61, Issue 2 (2012)

4. Nathan, B., Hai, Q., Neil, E., Ed, H., Taylor, R.: Physics-based Remaining Useful Life Prediction for Aircraft Engine Bearing Prognosis. Annual Conference of the Prognostics and Health Management Society (2009)

5. Shao, Y., Nezu, K.: Prognosis of Remaining Bearing Life Using Neural Networks. Proceedings of the Institution of Mechanical Engineers, Part I: Journal of Systems and Control Engineering, Volume 214, Issue 3 (2000)

6. Gebraeel, N., Lawley, M., Liu, R., Parmeshwaran, V.: Residual Life Predictions from Vibration-Based Degradation Signals: A Neural Network Approach. IEEE Transactions On Industrial Electronics, Volume 51, Issue 3 (2004)

7. Ghafari, S.H.: A Fault Diagnosis System for Rotary Machinery Supported by Rolling Element Bearings. PhD Thesis, University of Waterloo, Ontario, Canada, (2007)

20

8. Sutrisno, E., Oh, H., Vasan, A.S.S., Pecht, M.: Estimation of Remaining Useful Life of Ball Bearings Using Data Driven Methodologies. Prognostics and Health Management (PHM), IEEE Conference, DOI: 10.1109/ICPHM.2012.6299548 (2012)

9. Goebel, K., Saha, B., Saxena, A.: A Comparison of Three Data-Driven Techniques for Prognostics. 62nd Meeting of the Society for Machinery Failure Prevention Technology (2008)

10. Kim, H.E., Tan, A., C.C., Mathew, J., Kim, E., Y., H., Choi, B.K.: Machine Prognostics Based on Health State Estimation Using SVM. Proceedings of 3rd World Congress on Engineering Asset Management and Intelligent Maintenance Systems Conference, Volume 199 (2008)

11. Tian, Z.:, An Artificial Neural Network Method for Remaining Useful Life Prediction of Equipment Subject to Condition Monitoring. Journal of Intelligent Manufacturing, Springer, ISSN: 0956-5515, Volume 23, Issue 2, Online (2009)

12. Ben Ali, J., Chebel-Morello, B., Saidi, L., Malinowski, S., Fnaiech, F.: Accurate Bearing Remaining Useful Life Prediction Based on Weibull Distribution and Artificial Neural Network. Mechanical Systems and Signal Processing, Volumes 56–57 (2015)

13. Tobon-Mejia, D.A., Medjaher, K., Zerhouni, N., Tripot, G.: Estimation of the remaining useful life by using Wavelet Packet Decomposition and HMMs. Aerospace Conference, IEEE, DOI: 10.1109/AERO.2011.5747561 (2011)

14. Loutas, T.H., Roulias, D., Georgoulas, G.: Remaining Useful Life Estimation in Rolling Bearings Utilizing Data-Driven Probabilistic E-Support Vectors Regression. IEEE Transactions On Reliability, Volume 62, Issue 4 (2013)

15. Mba, D., Rao, R.B.K.N.: Development of Acoustic Emission Technology for Condition Monitoring and Diagnosis of Rotating Machines: Bearings, Pumps, Gearboxes, Engines, and Rotating Structures. The Shock and Vibration Digest (2006)

21

16. Jamaludin N., Mba, D., Bannister, R.H.: Condition Monitoring of Slow-Speed Rolling Element Bearings Using Stress Waves. Proceedings of the IMECHE, Part E, Journal of Process Mechanical Engineering, Volume 215, Issue 4 (2001)

17. Morhain, A., Mba, D.: Bearing Defect Diagnosis and Acoustic Emission. Proceedings of the IMECHE, Part J, Journal of Engineering Tribology, Volume 217, Issue 4 (2003)

18. Al-Ghamdi, A.M., Mba, D.: A Comparative Experimental Study on the Use of Acoustic Emission and Vibration Analysis for Bearing Defect Identification and Estimation of Defect Size. Mechanical Systems and Signal Processing, Volume 20, Issue 7 (2006)

19. Miettinen, J., Pataniitty, P.: Acoustic Emission in Monitoring Extremely Slowly Rotating Rolling Bearing. Proceedings of 12th International Congress on Condition Monitoring and Diagnostic Engineering Management, COMADEM, England (1999)

20. Choudhury, A., Tandon, N.: Application of Acoustic Emission Technique for the Detection of Defects in Rolling Element Bearings. Tribology International, Volume 33, Issue 1 (2000)

21. Price, E.D., Lees, A.W., Friswell, M.I.: Detection of Severe Sliding and Pitting Fatigue Wear Regimes Through the use of Broadband Acoustic Emission. IMechE Journal of Engineering Tribology, DOI: 10.1243/135065005X9817, Volume 219, Issue 2 (2005)

22. Yoshioka, T.: Detection of Rolling Contact Subsurface Fatigue Cracks Using Acoustic Emission Technique. Journal of the Society of Tribologists and Lubrication Engineers Volume 49, Issue 4 (1993)

23. Elforjani, M., Mba, D.: Monitoring the Onset and Propagation of Natural Degradation Process in a Slow Speed Rolling Element Bearing With Acoustic Emission. Journal of Vibration and Acoustics, DOI: 10.1115/1.2948413 (2008)

24. Elforjani, M., Mba, D.: Detecting the Onset, Propagation and Location of Non-Artificial Defects in a Slow Rotating Thrust Bearing with Acoustic Emission,

22

Insight Non-Destructive Testing and Condition Monitoring, DOI: 10.1784/insi.2008.50.5.264 (2008)

25. Elforjani, M., Mba, D.: Condition Monitoring of Slow Speed Shafts and Bearings with Acoustic Emission. Strain, Doi:10.1111/j.1475-1305.2010.00776.x (2011)

26. Elforjani, M., Mba, D.: Accelerated Natural Fault Diagnosis in Slow Speed Bearings with Acoustic Emission. Engineering Fracture Mechanics, Volume 77, Issue 1 (2010)

27. Murphy P.K.: Machine Learning A Probabilistic Perspective. MIT Press (2012)

28. Livingstone, J.D.: Artificial Neural Networks: Methods and Applications. Humana Press, 2009 Edition (2008)

29. Hopgood, A.A.: Intelligent Systems for Engineers and Scientists. CRC Press, 2nd Edition (2001)

30. Heaton, J.: Artificial Intelligence for Humans, Volume 3: Deep Learning and Neural Networks. CreateSpace Independent Publishing Platform (2015)

31. Apolloni, B., Bassis, S., Marinaro, M., Apolloni, B.: New Directions in Neural Networks. 18th Italian Workshop on Neural Networks, WIRN, Frontiers in Artificial Intelligence and Applications, Volume 193 (2009)

Figure 1 Test Bearing

Figure 2 Test Rig Layout
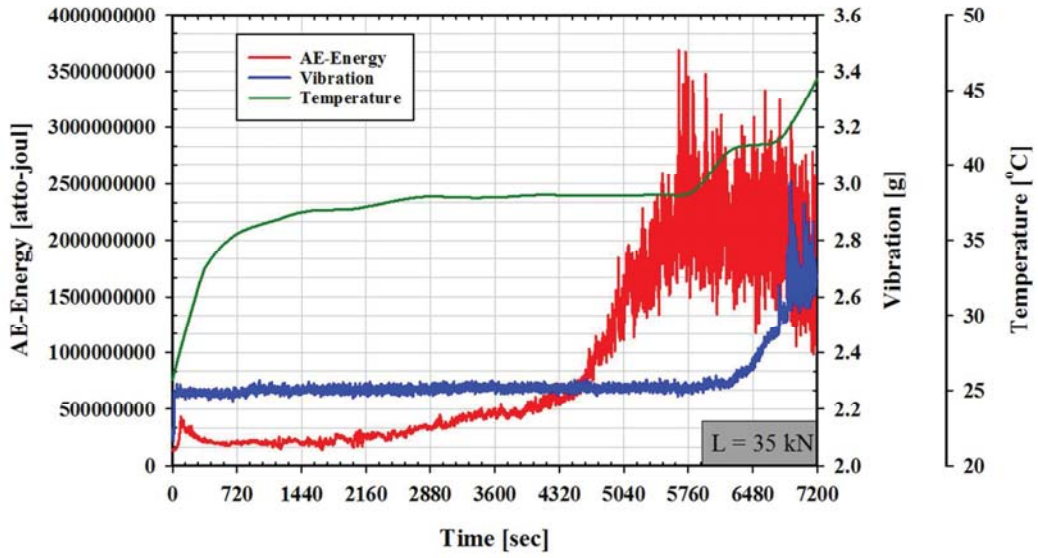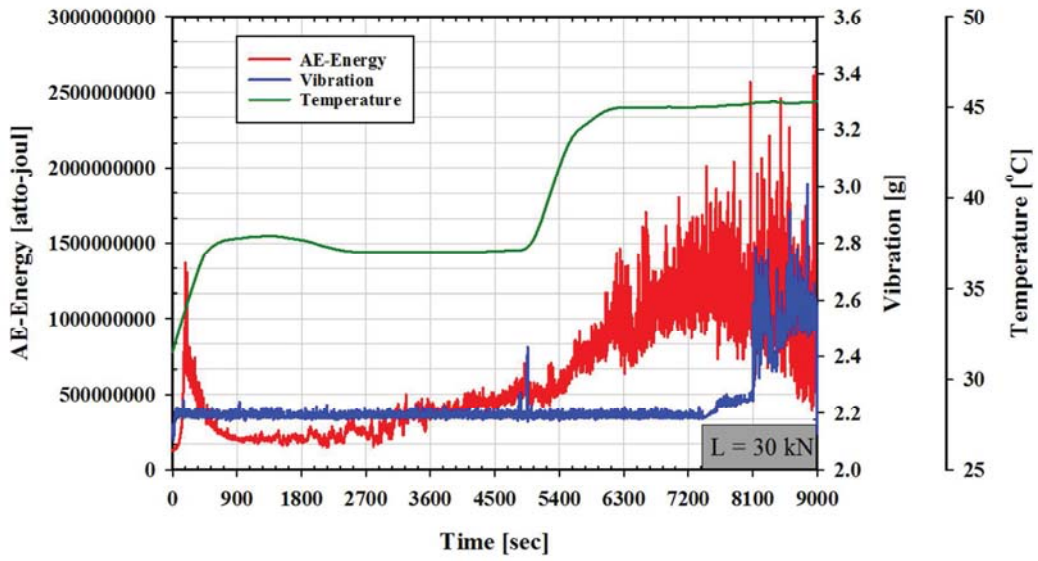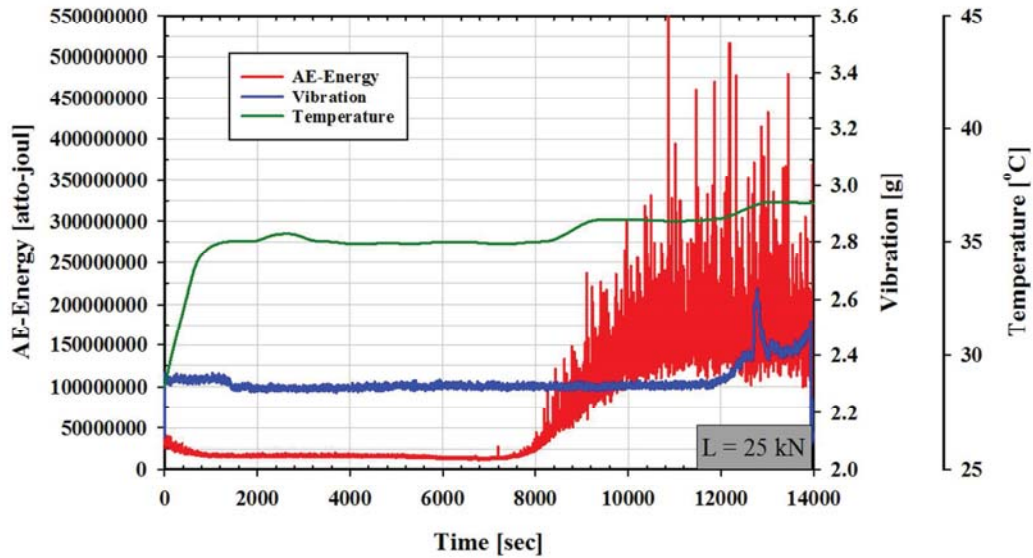
Figure 5 Test Conditions Case I (Load 35 kN)

Figure 4 Test Conditions Case II (Load 30 kN)
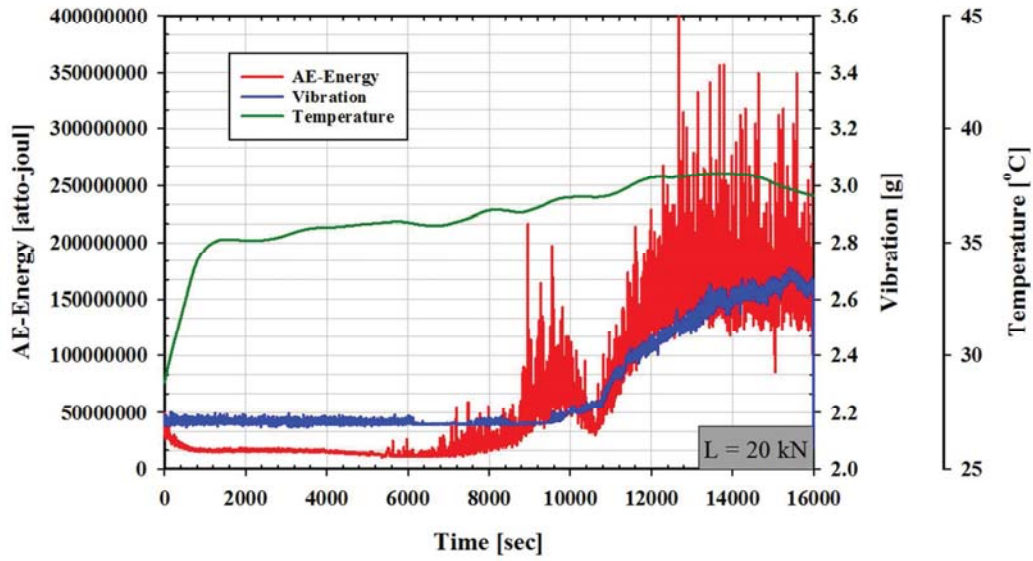
Figure 5 Test Conditions Case III (Load 25 kN)

Figure 6 Test Conditions Case IV (Load 20 kN)
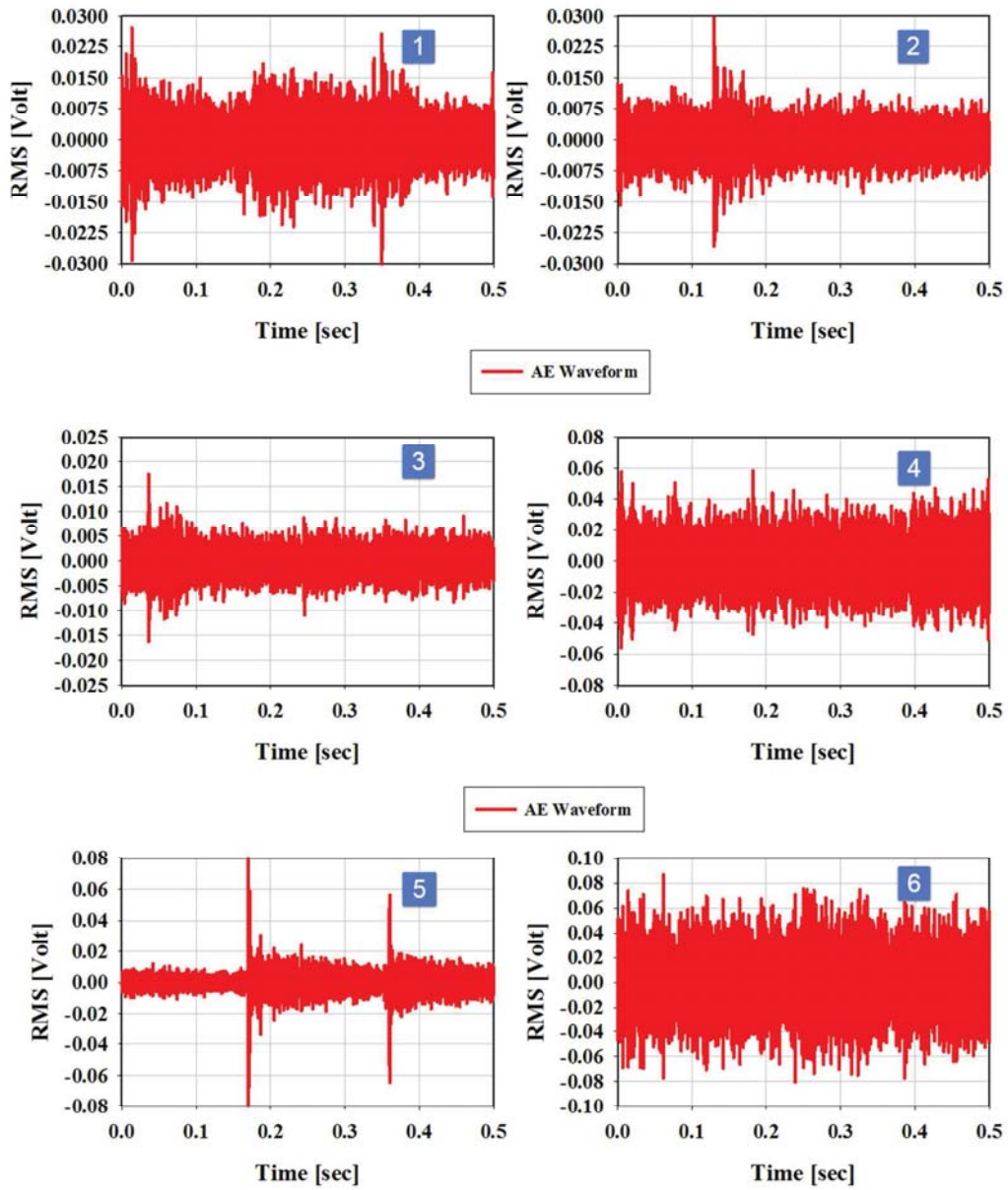
Figure 7 Surface Damage on the Bearing Cage

Figure 8 AE Waveforms associated with 35 kN Load (Onset Rise of AE Levels until the Termination)

Table 1 Correlation Analysis

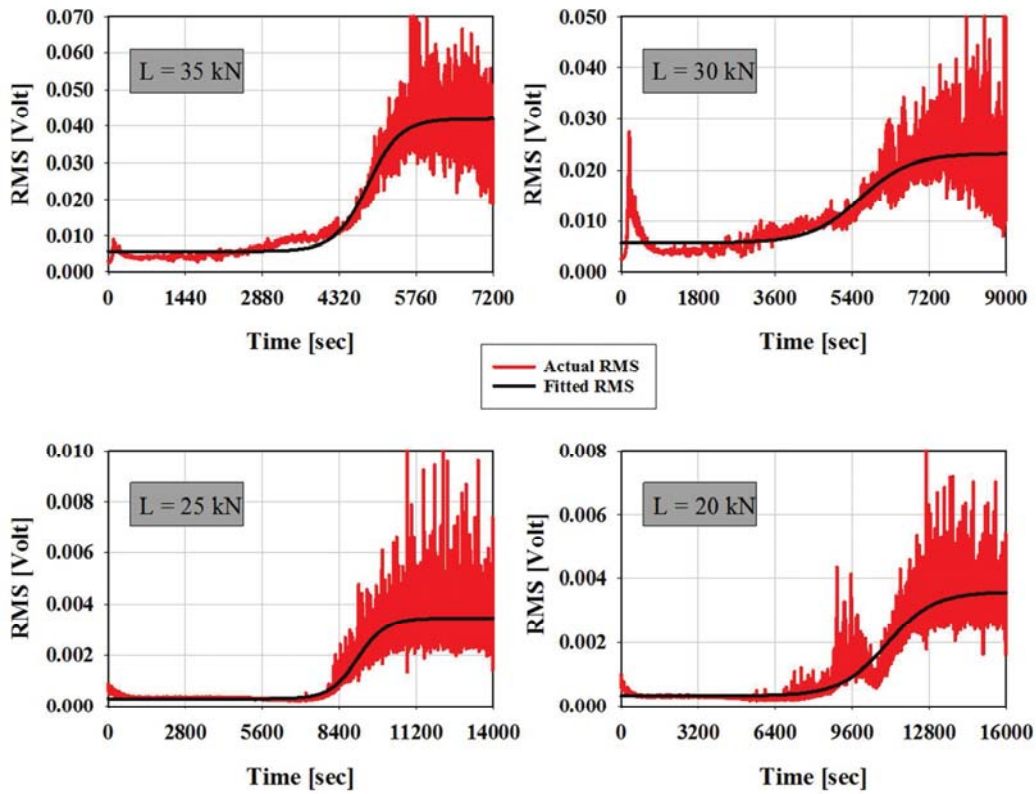| Pearson's Product-Moment Correlation				
Feature	t-test	p-value	95% Confidence Interval	Correlation Coefficient
SIE	22.92	2.2×10^{-16}	0.7760493 : 0.8568358	0.820498
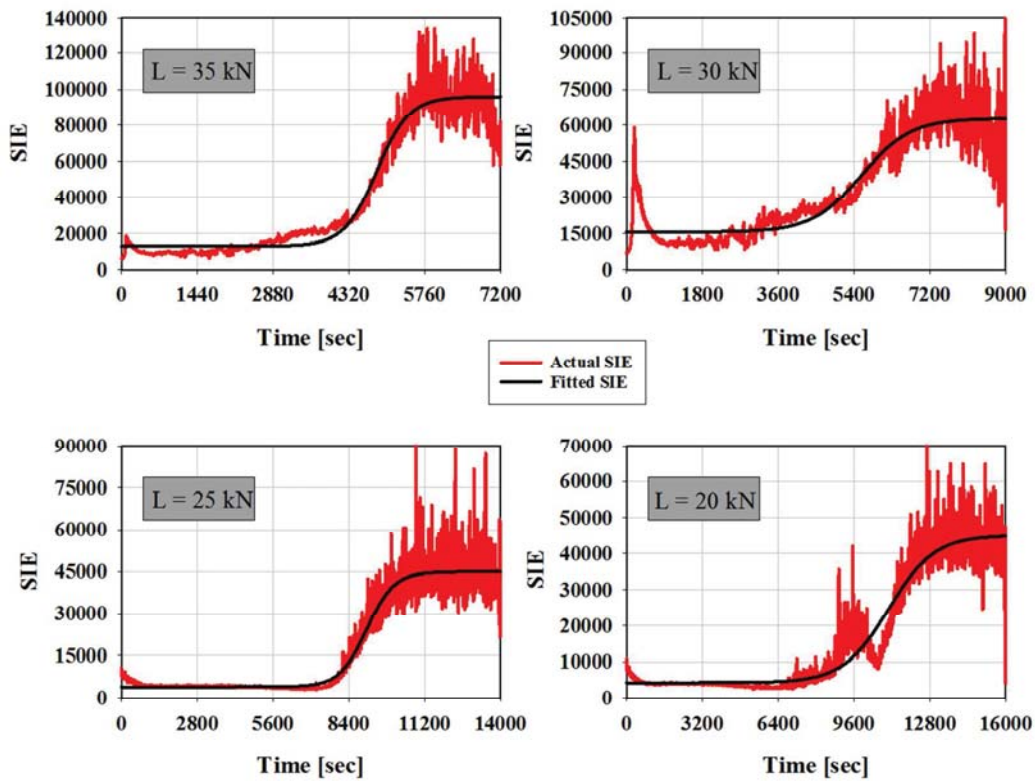
Figure 9 Actual and Fitted SIE

29

Figure 10 Actual and Fitted RMS

Table 2 Estimated Constants for the Exponential Model

Load (kN)	SIE				RMS			
	y_o	a	b	x_o	y_o	a	b	x_o
35	12942.18	83050.16	309.27	4851.73	0.0057	0.0363	308.08	4849.31
30	15432.17	47410.43	585.66	5579.44	0.0057	0.0175	592.80	5580.54
25	4047.15	40883.46	503.61	9073.62	0.0003	0.0031	506.03	9075.09
20	4295.43	40747.27	963.25	11072.94	0.0003	0.0032	969.40	11067.83

Table 3 Global Goodness of Fit for the Exponential Model

Load (kN)	SIE		RMS	
	R^2	$adj\ R^2$	R^2	$adj\ R^2$
35	0.9561	0.9561	0.9267	0.9266
30	0.8671	0.8669	0.8156	0.8155
25	0.9438	0.9437	0.8733	0.8732
20	0.9247	0.9246	0.8817	0.8817

30

1
2
3
4
5
6
7
8
9
10
11
12
13
14
15
16
17
18
19
20
21
22
23
24
25
26
27
28
29
30
31
32
33
34
35
36
37
38
39
40
41
42
43
44
45
46
47
48
49
50
51
52
53
54
55
56
57
58
59
60

Figure 11 Schematic of the Proposed ANN Model
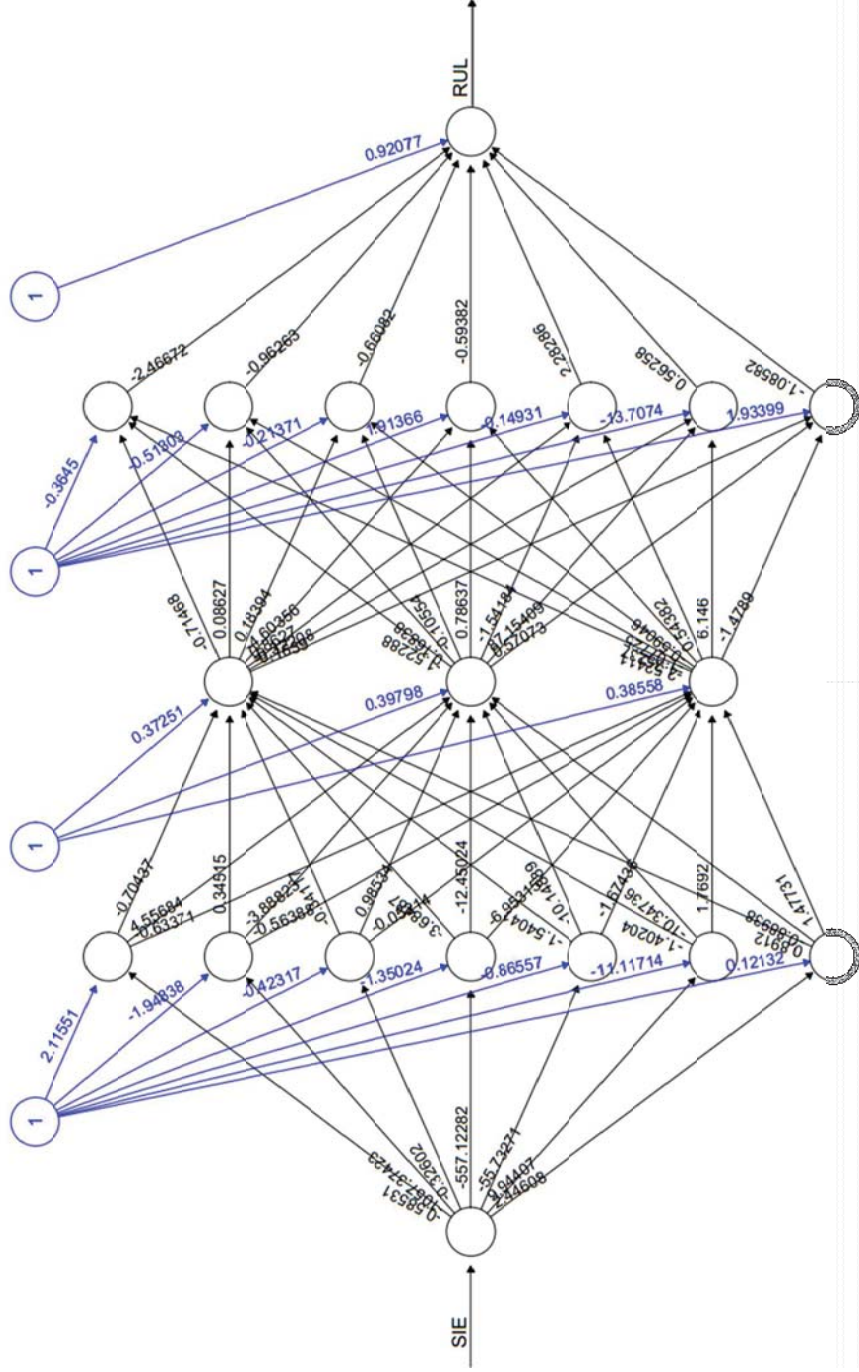
31

Structural Health Monitoring
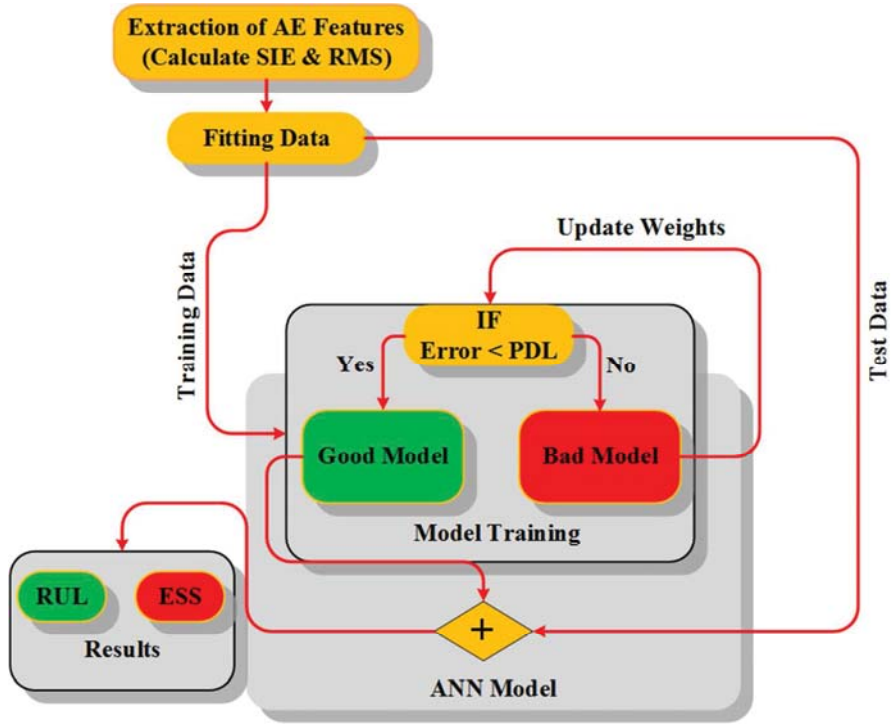
For Peer Review

1
2
3
4
5
6
7
8
9
10
11
12
13
14
15
16
17
18
19
20
21
22
23
24
25
26
27
28
29
30
31
32
33
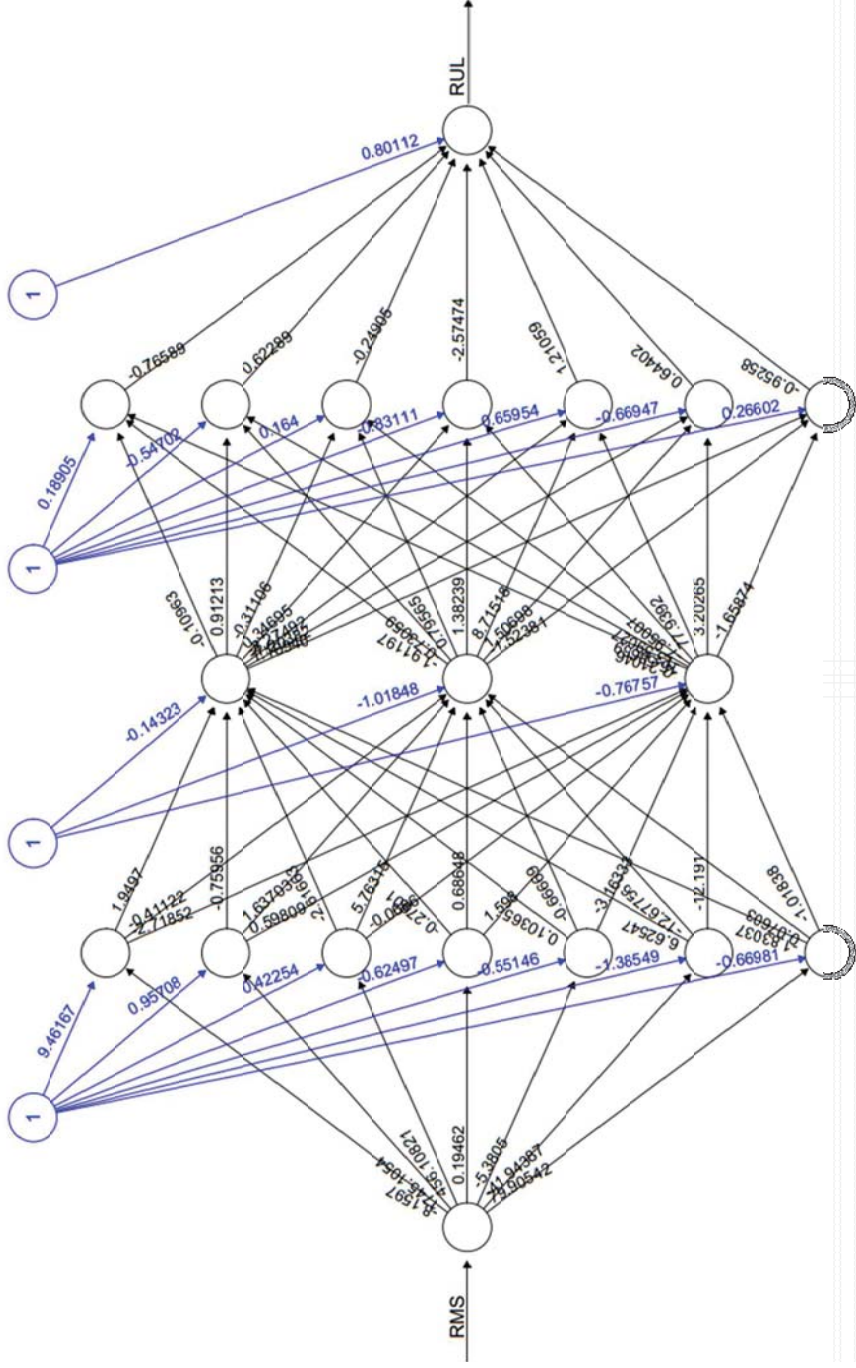34
35
36
37
38
39
40
41
42
43
44
45
46
47
48
49
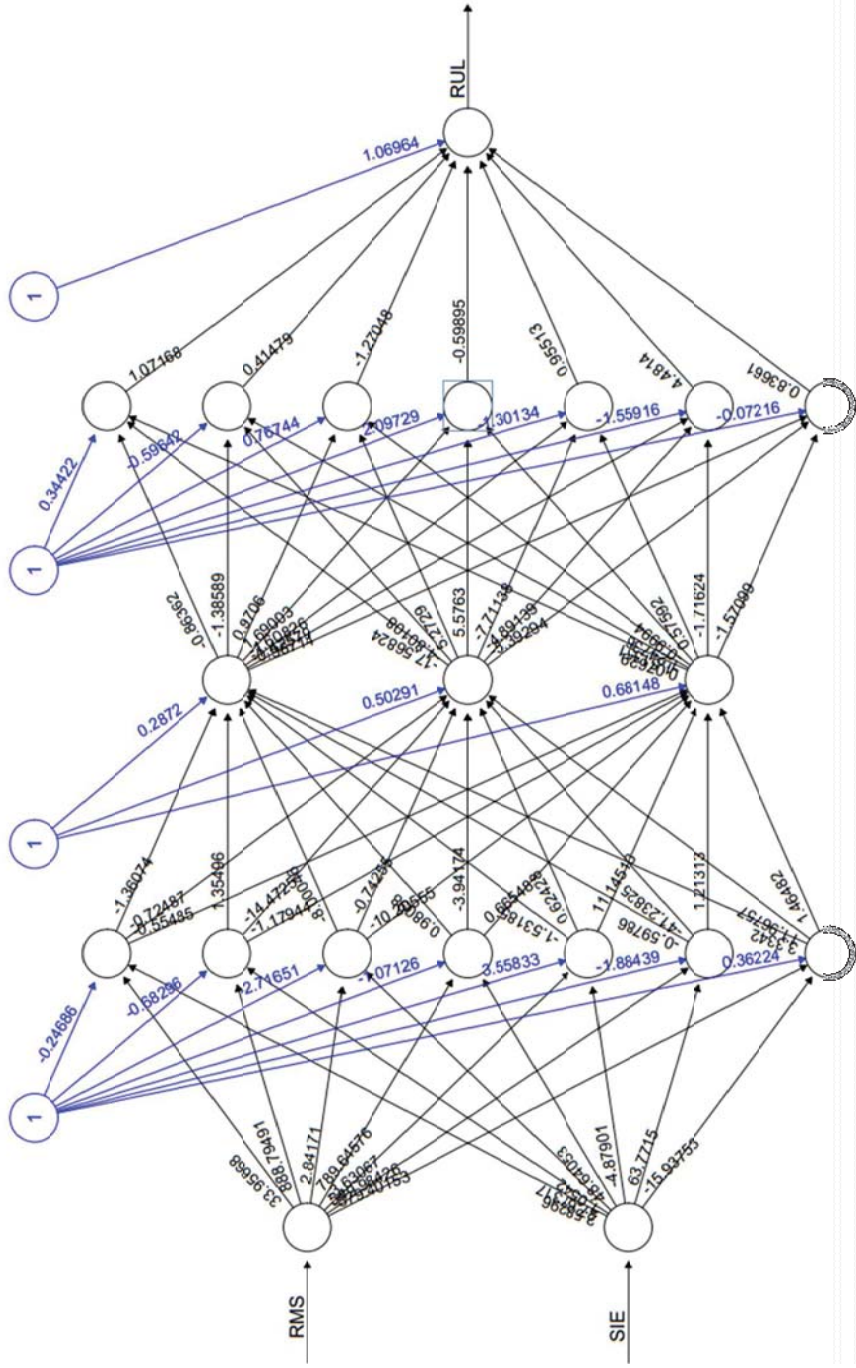
Error: 0.007923   Steps: 8887

Figure 12 ANN Structure (Two Inputs RMS & SIE)

33

Error: 0.004544   Steps: 13877

Figure 13 ANN Structure (One Input SIE)

34

Figure 14 ANN Structure (One Input RMS)

Error: 0.064202   Steps: 17584

35

1
2
3
4
5
6
7
8
9
10
11
12
13
14
15
16
17
18
19
20
21
22
23
24
25
26
27
28
29
30
31
32
33
34
35
36
37
38
39
40
41
42
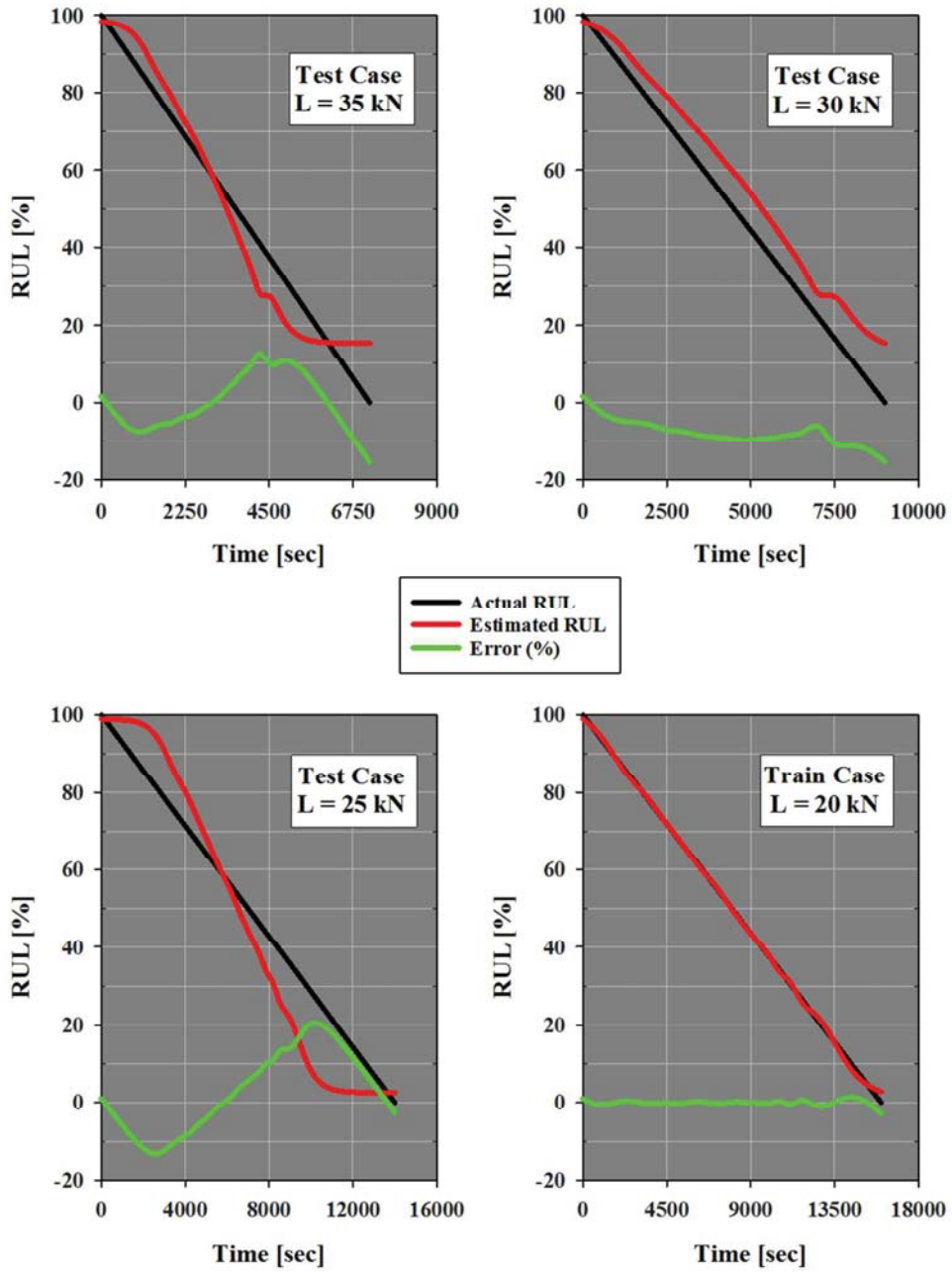43
44
45
46
47
48
49
50
51
52
53
54
55
56
57
58
59
60

1
2
3
4
5
6
7
8
9
10
11
12
13
14
15
16
17
18
19
20
21
22
23
24
25
26
27
28
29
30
31
32
33
34
35
36
37
38
39
40
41
42
43
44
45
46
47
48
49
50
51
52
53
54
55
56
57
58
59
60

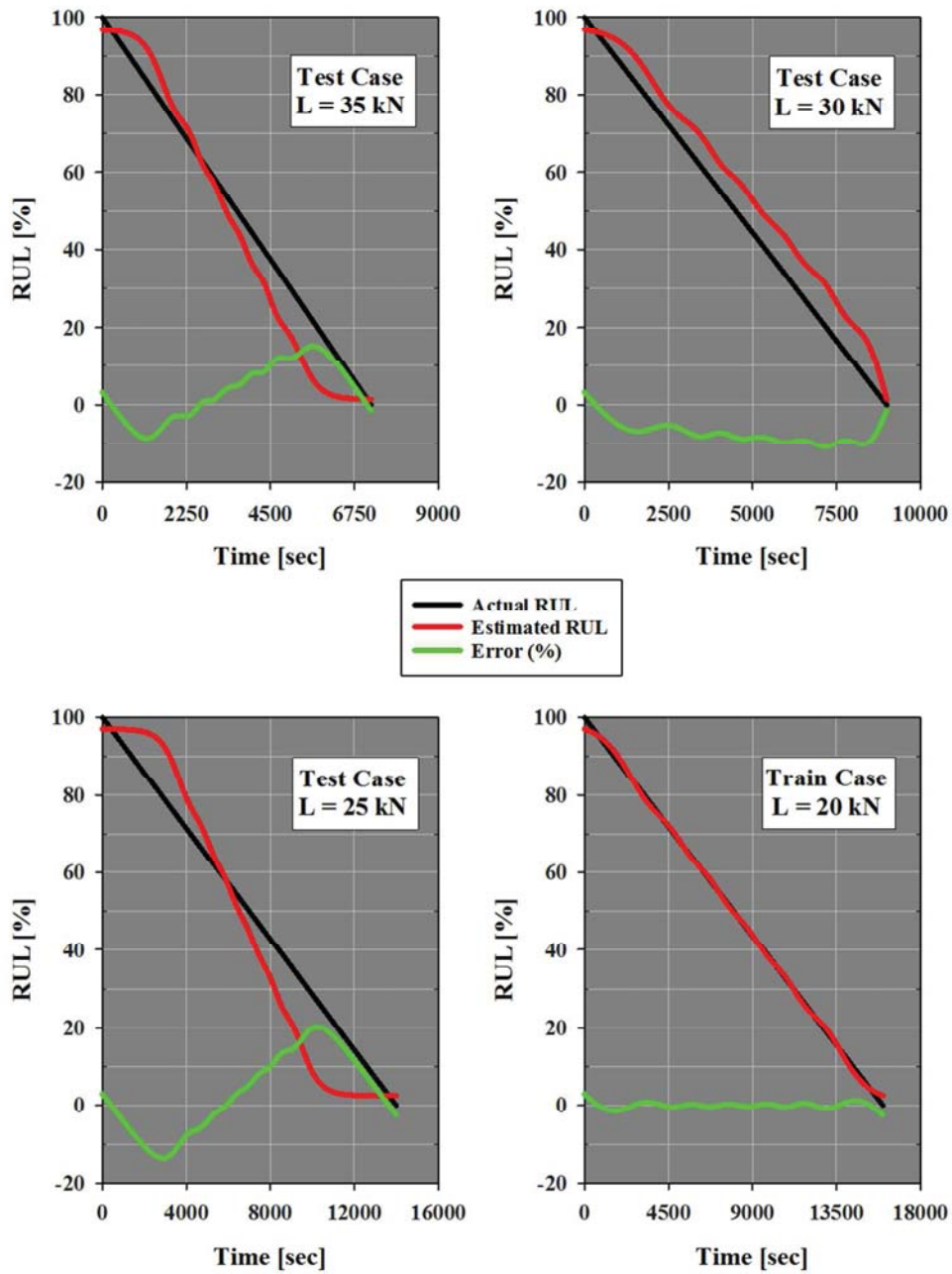**Figure 15 ANN Results (Two Inputs RMS & SIE)**

37

Figure 16 ANN Results (One Input SIE)

1
2
3
4
5
6
7
8
9
10
11
12
13
14
15
16
17
18
19
20
21
22
23
24
25
26
27
28
29
30
31
32
33
34
35
36
37
38
39
40
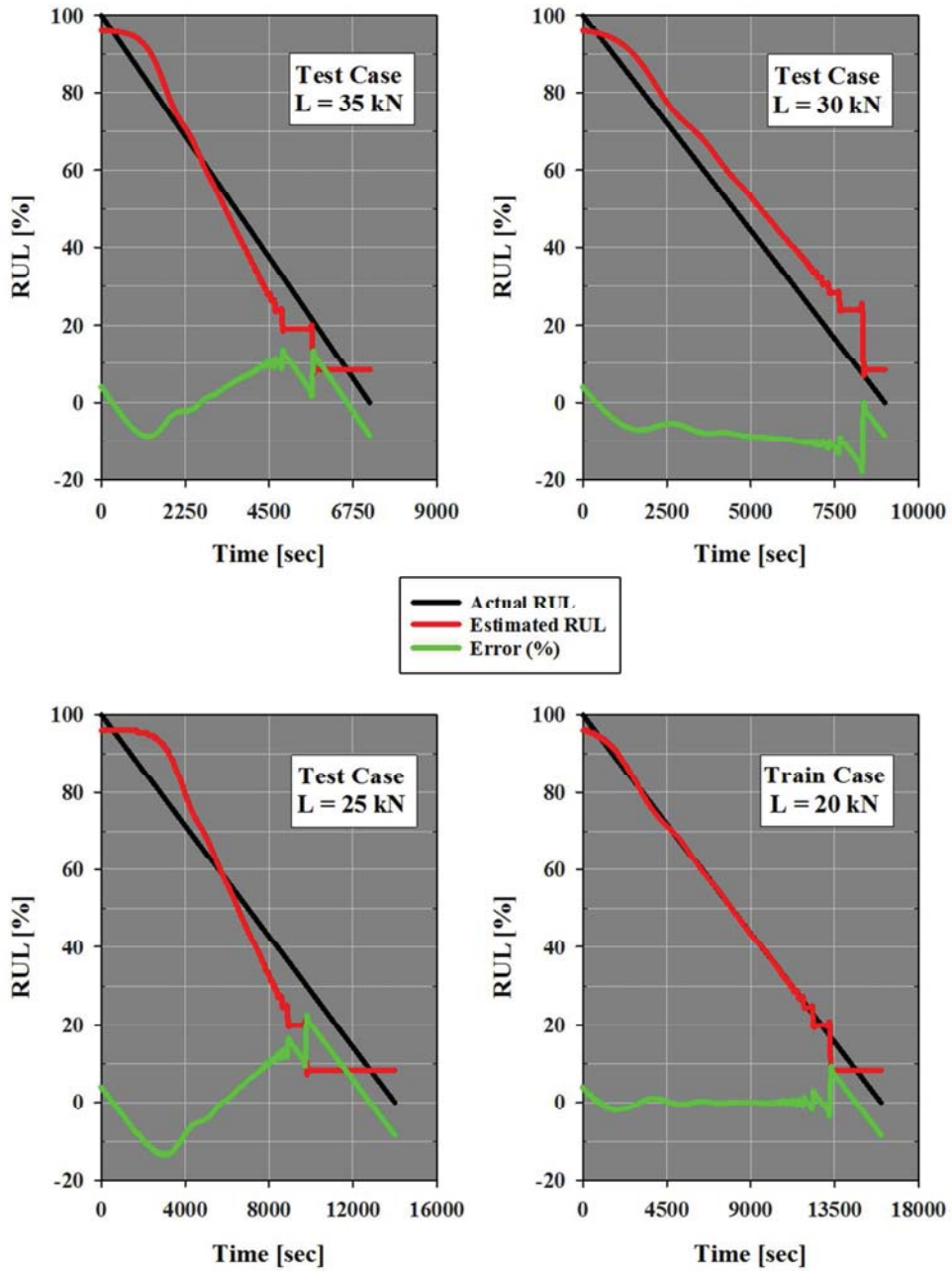41
42
43
44
45
46
47
48
49
50
51
52
53
54
55
56
57
58
59
60

Figure 17 ANN Results (One Input RMS)

Table 5 Error Results

Model Inputs	Error						
	ESS				Max (%)		
	35kN	30kN	25kN		35kN	30kN	25kN
RMS & SIE	6458	9020	15122		15.43	15.40	20.54
SIE	5237	7686	11457		13.38	10.58	20.30
RMS	8358	8526	14815		15.19	16.59	21.65